Supplementary Information

Capabilities of Automated LA-ICP-TOFMS Imaging of Geological Samples

Christoph Neff[1], Peter Keresztes Schmidt[1], Paolo S. Garofalo[2], Gunnar Schwarz[1,*], Detlef Günther[1,*]

[1] Laboratory of Inorganic Chemistry, Department of Chemistry and Applied Biosciences, ETH Zurich, Vladimir-Prelog-Weg 1, 8093 Zürich, Switzerland
[2] Università degli Studi di Bologna, Dipartimento di Scienze Biologiche, Geologiche ed Ambientali, Via Zamboni 67, 40126 Bologna, Italy

* corresponding authors: detlef.guenther@sl.ethz.ch, schwarz@inorg.chem.ethz.ch

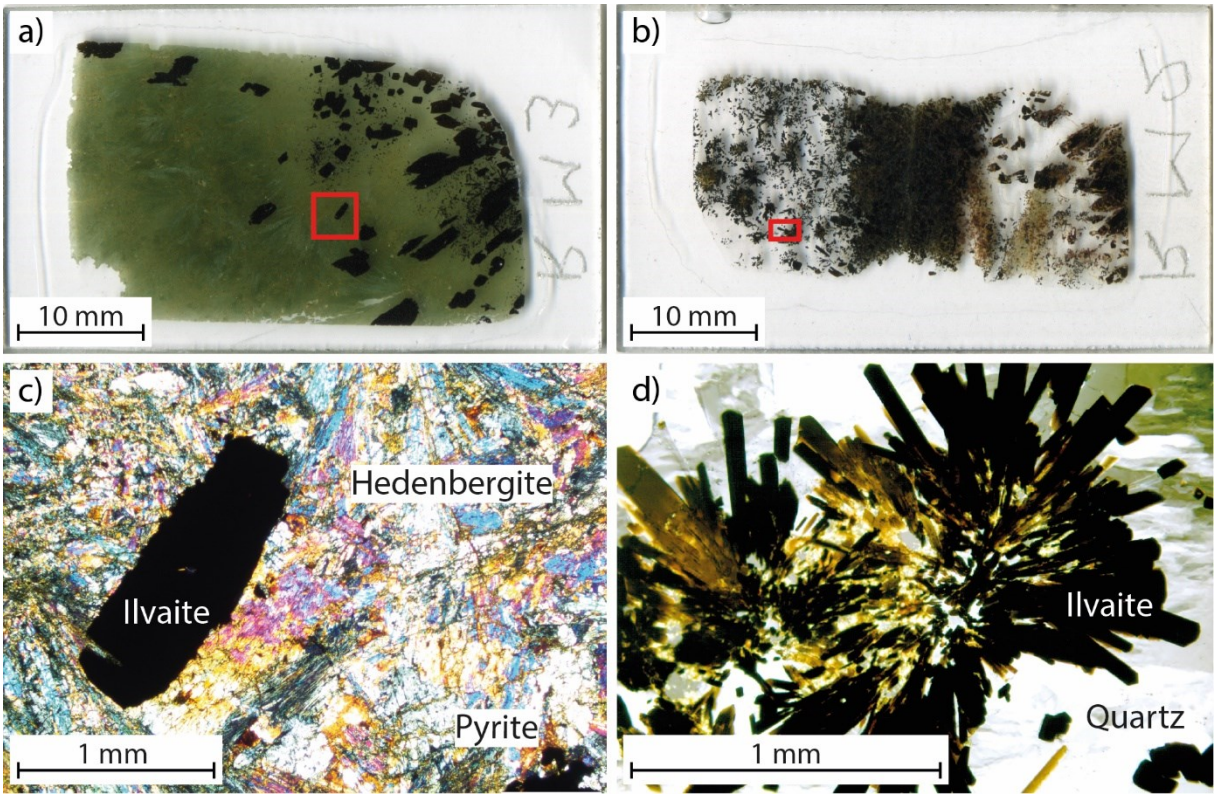

Fig. S1 Polished petrographic thin sections of sample RM3 (a) and RM2 (b) used for this study. The red areas in a) and b) mark the imaged areas of Fig. 2 and Fig. 4. c) Large and well crystallized ilvaite prism set in fibrous, elongated hedenbergite (transmitted light petrographic image, crossed nicols). Relatively small, euhedral pyrite crystals form between hedenbergite. d) Large and well crystallized, rosette-like aggregates of ilvaite set in quartz crystals and equivalent to those analyzed here (transmitted light petrographic image, parallel nicols). Notice that ilvaite is almost invariably opaque in the samples.

TOFMS data structure and triggering strategy for element imaging

When in operation, the ICP-TOFMS (icpTOF2R, Tofwerk AG, Thun, Switzerland) is constantly running with an ion extraction and spectra acquisition rate of 21739 kHz. Only whether data is recorded is due to the user and settings. Sustained continuous data acquisition (i.e. recording) is possible at a frequency of 943 Hz (23 TOFMS extractions per mass spectrum), this is limited by data transfer from the analog-to-digital converter to the computer hard drive.[1]

Previously, we acquired large images by continuously acquiring data ("free running ICP-TOFMS") and only triggered subsections of several consecutive lines manually or using an automated 'write trigger' either at the start or end of acquiring data files to the imaging control computer to start a new subsection.[2-5] The following section provides a description of the utilization of the TOFMS data structure for LA-ICP-TOFMS element imaging. The terminology for data structure follows mostly the ICP-TOFMS vendor (Tofwerk AG, Thun, Switzerland).

ICP-TOFMS data is stored in a HDF5 data file format. Inherently, mass spectra resulting from averaging multiple ion extractions are stored in segments. While it is also possible to store data from mass spectra of individual ion extractions, this is not possible in a sustained continuous manner, i.e. in most cases only averaged spectra can be accessed subsequently. The number of averaged mass spectra into a segment yields the temporal resolution of the data. The smaller

the number of mass spectra per segment the more data points are accessible for the same transient signal for an individual laser pulse, while in principle, only a single segment may be sufficient. Segments are collected in blocks and transferred from the analog-to-digital converter to the memory, which cannot be accessed individually, in the ICP-TOFMS computer. There, data is handled in bufs and writes as additional dimensions of the resulting HDF5 data file. The data structure poses several restrictions to the user. For instance, the number of segments times the number of bufs stored in a write cannot exceed 1250 and commonly each block contains one segment and each memory contains one block. In our case, the length of one line is restricted to 1250 pixel if one segment per pixel is recorded. Nevertheless, this structure allows data to be stored in different dimensions, separation of data for individual sample positions, and ordered by relative coordinates and implement a convenient triggering scheme for automation and image data acquisition control.

We used external triggering of blocks in conjunction with laser pulses and included a delay to allow for aerosol transport from the sample to the plasma to initiate data acquisition for individual pixels. The delay is determined for each experiment individually to account for differences in gas flows. Moreover, the actual separation of laser and block triggers permitted to not trigger data acquisition for cleaning pulses. This results in a buf containing data for individual pixels and the transient signal from the aerosol originating from the corresponding sample position, while different averaged spectra, i.e. data points, across the transient signals remain accessible. Further down, bufs are pooled into writes. In our approach for acquiring imaging data for rectangular images, the number of bufs in a write corresponds with the number of pixels in a line (of a subsection) and therefore each write contains the data of a single line (of a subsection). Writes are the data dimension which is finally written into the file on the hard drive. Data from incomplete writes at the end of a file are not recorded. A set number of writes is collected to make up each data file. To acquire large images, multiple subsections positioned next to each other were used, which were stitched together subsequently during data processing. To initiate the next subsection, at the end of the last write of a subsection the icpTOF2R sends a trigger signal to the imaging control computer (Fig. S2). This results in a fully coordinated operation of translational stage for sample positioning, laser pulse delivery, and data acquisition by the ICP-TOFMS.

While it is not necessary to acquire more than one segment per pixel and it would reduce the data file size substantially, this also reduces the amount of data available for later inspection, e.g. signal separation, to distinguish between increased background signal and signal from individual ablations. Furthermore, in HD mode it is often not necessary to acquire at such a high temporal resolution to distinguish between aerosol signals from different laser pulses, but to represent the overall transient signals in order to recognize as the case may be inhomogeneity in depth for voxels.

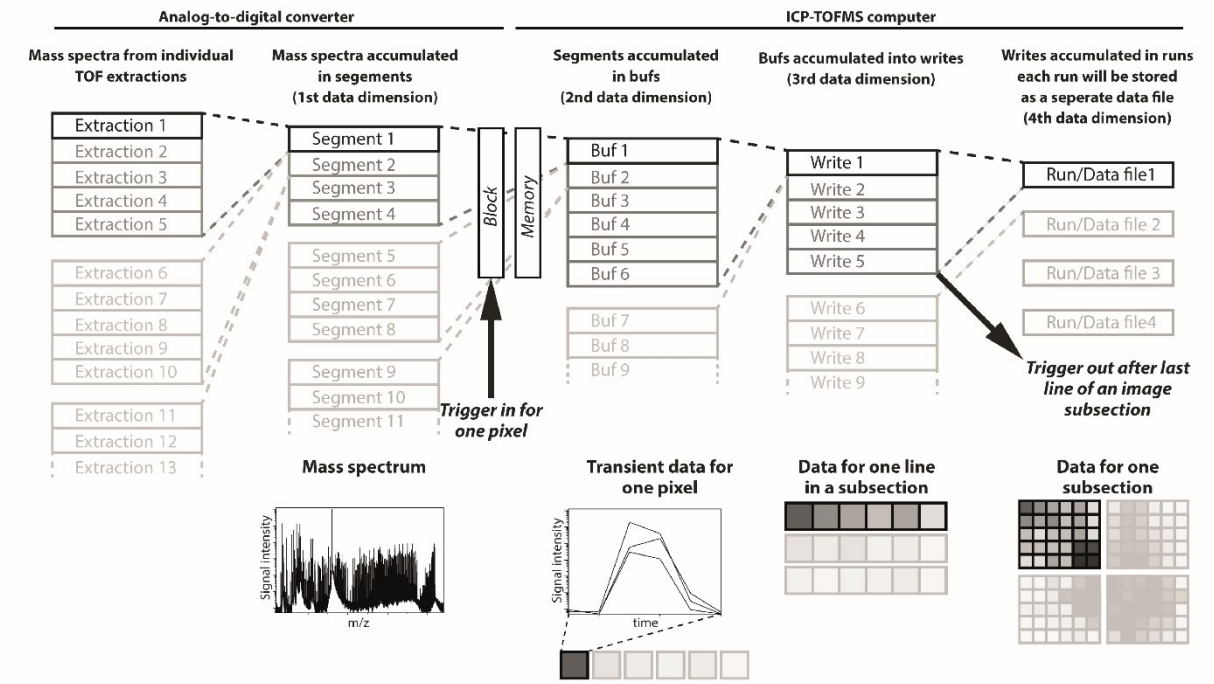

Fig. S2 The data structure of LA-ICP-TOFMS imaging for rectangular areas applied in this study. The arrows indicate trigger signals to the ICP-TOFMS to acquire data for a single pixel (block trigger) or from the ICP-TOFMS to start a new subsection of a larger image after a defined number of writes.

Table S1: Pixel LOD for ablation modes HD, SP and OL for NIST SRM 610.

	Pixel LOD [mg/kg]				Pixel LOD [mg/kg]		
Isotope	HD	SP	OL	Isotope	HD	SP	OL
^{23}Na	300	1000	300	^{115}In	0.3	4	0.3
^{25}Mg	70	800	60	^{118}Sn	3	20	3
^{27}Al	10	100	10	^{121}Sb	1	10	1
^{29}Si	3000	10000	3000	^{125}Te	10	200	10
^{31}P	100	700	100	^{133}Cs	0.4	4	0.4
^{39}K	300	600	300	^{137}Ba	3	30	3
^{44}Ca	200	1000	200	^{139}La	0.3	3	0.3
^{45}Sc	3	30	3	^{140}Ce	0.3	3	0.3
^{49}Ti	50	500	50	^{141}Pr	0.3	3	0.2
^{51}V	2	20	2	^{146}Nd	1	20	1
^{52}Cr	10	40	9	^{147}Sm	2	20	2
^{55}Mn	50	500	50	^{153}Eu	0.4	5	0.4
^{56}Fe	300	1000	300	^{157}Gd	1	20	1
^{59}Co	3	30	3	^{159}Tb	0.2	3	0.2
^{60}Ni	8	90	8	^{163}Dy	0.9	10	0.8
^{65}Cu	9	80	9	^{165}Ho	0.2	3	0.2
^{66}Zn	10	100	10	^{166}Er	0.7	10	0.6
^{71}Ga	5	70	6	^{169}Tm	0.2	3	0.2
^{74}Ge	30	400	40	^{172}Yb	1	10	0.9
^{75}As	100	800	100	^{175}Lu	0.2	3	0.2
^{77}Se	300	3000	300	^{178}Hf	0.7	10	0.7
^{85}Rb	2	10	2	^{181}Ta	0.2	3	0.2
^{88}Sr	0.7	6	0.6	^{182}W	1	10	1
^{89}Y	0.5	7	0.5	^{185}Re	0.6	8	0.6
^{90}Zr	0.9	10	0.9	^{195}Pt	1	20	1
^{93}Nb	0.5	5	0.4	^{197}Au	0.7	9	0.7
^{95}Mo	3	30	3	^{205}Tl	0.4	5	0.5
^{103}Rh	0.4	5	0.4	^{208}Pb	0.6	7	0.7
^{105}Pd	1	10	0.9	^{209}Bi	0.4	5	0.5
^{107}Ag	2	10	2	^{232}Th	0.3	4	0.2
^{111}Cd	7	70	9	^{238}U	0.3	3	0.3

References

1. Hendriks, L., A. Gundlach-Graham, B. Hattendorf, and D. Guther, *Characterization of a new ICP-TOFMS instrument with continuous and discrete introduction of solutions.* Journal of Analytical Atomic Spectrometry, 2017. **32**(3): p. 548-561.

2. Burger, M., A. Gundlach-Graham, S. Allner, G. Schwarz, H.A.O. Wang, L. Gyr, S. Burgener, B. Hattendorf, D. Grolimund, and D. Günther, *High-Speed, High-Resolution, Multielemental LA-ICP-TOFMS Imaging: Part II. Critical Evaluation of Quantitative Three-Dimensional Imaging of Major, Minor, and Trace Elements in Geological Samples.* Analytical Chemistry, 2015. **87**(16): p. 8259-8267.
3. Burger, M., G. Schwarz, A. Gundlach-Graham, D. Kaser, B. Hattendorf, and D. Gunther, *Capabilities of laser ablation inductively coupled plasma time-of-flight mass spectrometry.* Journal of Analytical Atomic Spectrometry, 2017. **32**(10): p. 1946-1959.
4. Gundlach-Graham, A., M. Burger, S. Allner, G. Schwarz, H.A.O. Wang, L. Gyr, D. Grolimund, B. Hattendorf, and D. Günther, *High-Speed, High-Resolution, Multielemental Laser Ablation-Inductively Coupled Plasma-Time-of-Flight Mass Spectrometry Imaging: Part I. Instrumentation and Two-Dimensional Imaging of Geological Samples.* Analytical Chemistry, 2015. **87**(16): p. 8250-8258.
5. Gundlach-Graham, A., P.S. Garofalo, G. Schwarz, D. Redi, and D. Günther, *High-resolution, Quantitative Element Imaging of an Upper Crust, Low-angle Cataclasite (Zuccale Fault, Northern Apennines) by Laser Ablation ICP Time-of-Flight Mass Spectrometry.* Geostandards and Geoanalytical Research, 2018. **42**(4): p. 559-574.